International Journal of Solids and Structures 41 (2004) 1411–1433

INTERNATIONAL JOURNAL OF SOLIDS and STRUCTURES

www.elsevier.com/locate/ijsolstr

Approximate analysis of building structures with identical stories subjected to earthquakes

Gabriella Tarján [a,*], László P. Kollár [b,1]

[a] Research Group for Computational Structural Mechanics, Department of Structural Mechanics, Budapest University of Technology and Economics, Mûegyetem rkpt. 3. Kmf 35, 1521 Budapest, Hungary

[b] Department of Mechanics, Materials and Structures, Budapest University of Technology and Economics, Mûegyetem rkpt. 1, 1521 Budapest, Hungary

Received 9 May 2003; received in revised form 15 October 2003

Abstract

In this paper an approximate earthquake analysis is presented for multistory building structures. The building is stiffened by an arbitrary combination of lateral load-resisting subsystems (shear walls, frames, trusses, coupled shear walls, cores). We consider stories with identical stiffnesses and masses, however the mass at the top floor may be different. The analysis is based on the continuum method. The spatial vibration problem of the replacement beam is solved approximately. Simple formulas are given to calculate the periods of vibration and internal forces of a building structure subjected to earthquakes.

The utility and accuracy of the method is demonstrated by two numerical examples, in which the approximate solution is compared with finite element calculations.

Keywords: Eigenfrequency; Internal forces; Spatial vibration; Approximate analysis; Building

1. Introduction

During an earthquake damage to buildings is largely caused by dynamic loads. Therefore, to design buildings resistant to earthquakes, the dynamic characteristics of the building must be known. The important characteristics, such as circular frequencies and mode shapes can be calculated by numerical means, such as finite element methods. While such methods are necessary for final design, approximate analysis are most helpful in preliminary design. Analytical tools shed light on the use of different structural elements and on their dimensions. This type of information can greatly facilitate the numerical calculations, leading to computational efficiency and savings in effort and time. Analytical results are also useful in verifying numerical results, a necessary step when using complex computer codes.

* Corresponding author. Tel.: +36-1-463-16-61; fax: +36-14631099.

E-mail addresses: gtarjan@hotmail.com (G. Tarján), lkollar@eik.bme.hu (L.P. Kollár).

[1] Tel.: +36-1-463-1317; fax: +36-1-463-1773.

0020-7683/$ - see front matter
doi:10.1016/j.ijsolstr.2003.10.021

Recognizing the importance of analytical approaches, many investigators have presented analytical solutions for the response of buildings to dynamic loads.

The most widely used approximate calculations are based on the ‘‘continuum method’’ (Hegedűs and Kollár, 1999; Skattum, 1971; Stafford Smith and Coull, 1991; Szerémi, 1978; Zalka, 1993, 1994, 2000), when the stiffened building structures is replaced by a (continuous) beam. Several authors applied the continuum models to calculate the dynamic characteristics of building structures stiffened by one or several lateral load-resisting subsystems, which vibrate in a symmetry plane (plane problem) or undergo lateral–torsional vibration (spatial problem).

Skattum (1971) solved the differential equation of the lateral vibration of one load-resisting subsystem and presented the results in a number of figures, however his results are too tedious for design purposes. Basu (1983), Basu et al. (1984) and Kollár (1991) gave design charts for the *circular frequency*, however their results are limited for not slender buildings. Rosman gave design charts for the circular frequency of several lateral load-resisting subsystems. His results are applicable for bracing systems consisting of shear walls and slender frames. L. Kollár (who is not the author of this article) and Iványi (Kollár and Iványi, 1966) presented an approximate expression for the circular frequency of frame structures, the accuracy of which (for a 10 story building) is between −16% and +30% (Köpecsiri, 1997). Rutenberg (1975, 1979) and Stafford Smith and Crowe (1986) worked out explicit expressions for the lateral vibration of one or several lateral load-resisting subsystem, however these solutions are limited for a certain parameter range (Potzta, 2002; Stafford Smith and Yoon, 1991). Ng and Kuang (2000) presented the solution of lateral and lateral–torsional vibration of one or several lateral load-resisting subsystems, however they neglected the compressibility of columns. Zalka (2001) and Köpecsiri and Kollár (1999a,b) derived expressions for the

Table 1
Summary of methods available in the literature to calculate the dynamic characteristics of replacement beams

Author\subsystem	Circular frequency				Remark	Internal forces				Remark
	Plane problem		Spatial problem			Plane problem		Spatial problem		
	One	Several	One	Several		One	Several	One	Several	
Skattum (Skattum, 1971)	√	–	–	–	Charts	(√)	–	–	–	Charts
Basu (Basu, 1983; Basu et al., 1984), Kollár (Kollár, 1991)	(√)	–	–	–	Charts	(√)	–	–	–	Charts
Rosman (Rosman, 1974), (Rosman, 1973)	(√)	(√)	–	–	Charts	–	–	–	–	–
L. Kollár (Kollár and Iványi, 1966)	(√)	(√)	–	–	Expression	–	–	–	–	–
Rutenberg (Rutenberg, 1975, 1979)	(√)	(√)	–	–	Expressions	–	–	–	–	–
Stafford Smith and Crowe (Stafford Smith and Crowe, 1986)	(√)	(√)	–	–	Expressions	–	–	–	–	Charts
Stafford Smith and Yoon (Stafford Smith and Yoon, 1991)	–	–	–	–	Expressions	(√)	(√)	–	–	Charts
Ng (Ng and Kuang, 2000)	(√)	(√)	(√)	(√)	Expression	–	–	–	–	–
Zalka (Zalka, 2001)	√	√	√	√	Table	–	–	–	–	–
Köpecsiri (Köpecsiri and Kollár, 1999a,b)	√	√	√	√	Expression	√	–	–	–	–
Present article	√	√	√	√	Expression	√	√	√	√	–

The parentheses mean that the results are applicable only for a parameter range.

circular frequency which has general applicability. The error of Köpecsiri's formula in the first circular frequency is between 0% and −16%. Zalka improved the accuracy of the case when the compressibility of the columns are negligible, however, in general, the accuracy of his solution is between −16% and +16%. (In Section 5 we present an approximate calculation for circular frequency of lateral or lateral–torsional vibration of one or several lateral load-resisting subsystems. The error in the first circular frequency of in-plane vibration is between −2.3% and +2.3%).

To calculate the *base internal forces* arising from earthquakes we can find solutions only for lateral vibration of one lateral load-resisting subsystem. Skattum (1971) determined the mode shapes of lateral vibration, however he did not present the calculation of the earthquake forces. Basu (1983) and Basu et al. (1984) gave design charts to calculate the base shear force when the compressibility of the columns are negligible. Stafford Smith and Yoon (1991) worked out approximate formula to calculate the base shear force also using design charts. His solution is not applicable for tall rigid frames and braced frames. Köpecsiri and Kollár (1999a,b) gave expression for base shear and for overturning moment. (In Section 6 we present an approximate calculation for base internal forces of lateral or lateral–torsional vibration of one or several lateral load-resisting subsystems.)

The aforementioned analytical investigations are summarized in Table 1. It is seen that none of the previous solutions provides the base internal forces in torsional vibration. In this paper methods are presented for calculating these parameters. In addition, method is given for calculating the circular frequencies without the need of design tables.

2. Problem statement

We consider a building structure which contains an arbitrary combination of lateral load-resisting subsystems, i.e. shear walls, coupled shear walls, frames, trusses and cores. The arrangement of the stiffening system is either symmetrical or arbitrary (Fig. 1).

The arrangement of the lateral load-resisting subsystems is identical at each floor. The dimensions and stiffnesses at every story are also identical, the masses of the individual floors and their horizontal distributions are the same except at the top floor. (Uniform mass distribution represents a building with the same concentrated mass at every story (mh, where m is the mass per unit height and h is the story height) except the top floor, where the concentrated mass is $\frac{mh}{2}$. In most practical cases the top floor has the same concentrated mass as the other floors, thus we extend the analysis taking a concentrated mass at the top into account.)

Our aim is to develop simple approximate expressions for the calculation of the eigenfrequencies, and of the seismic forces.

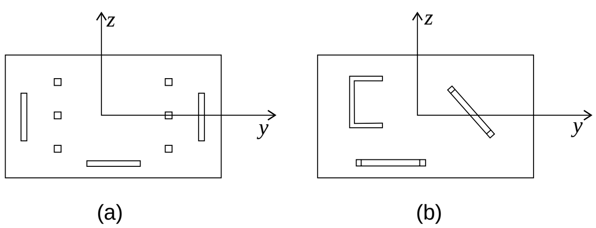

Fig. 1. Symmetrical (a) and unsymmetrical (b) arrangements of the lateral load-resisting subsystems.

3. Basic assumptions, approach

We assume that the material behaves in a linearly elastic manner.

The floors are considered to be rigid in their plane and they transfer only horizontal forces to the lateral load-resisting subsystems. In addition, we assume that the floors connect the stiffening system "continuously", hence each cross-section of the building remains undeformed in the horizontal plane.

We apply the continuum method with the replacement beam developed in Potzta and Kollár (2003) to obtain the eigenfrequencies and the mode shapes. The formulas to determine the stiffnesses of the replacement beam are also given in Potzta and Kollár (2003).

We formulated the differential equation of the freely vibrating replacement beam and solved when the bottom is built-in and the top is free (Potzta, 2002), however these results are still too tedious for design purposes and require the use of design charts or complicated expressions. To overcome these shortcomings we use approximate solutions of the continuum with the aid of the following three theorems, which are illustrated in Fig. 2.

Dunkerley's theorem (Bishop and Jonson, 1960; Dunkerley, 1984): The structure contains two sets of masses denoted by M_1 and M_2. The circular frequency of the structure can be approximated by $1/\omega^2 = 1/\omega_1^2 + 1/\omega_2^2$, where ω_1 is the circular frequency of the structure if M_2 is set equal to zero while ω_2 is the circular frequency if M_1 is set equal to zero.

Southwell's theorem (Bishop and Jonson, 1960; Lamb and Southwell, 1921): The structure is characterized by two stiffnesses, denoted by D_1 and D_2, such that if we set either one of the stiffnesses equal to infinity the structure would become infinitely rigid. The circular frequency can be approximated by $\omega^2 = \omega_1^2 + \omega_2^2$, where ω_1 is the circular frequency of the structure if D_2 is set equal to zero while ω_2 is the circular frequency if D_1 is set equal to zero.

Föppl's theorem: Föppl's theorem was developed for the stability analysis of elastic structures (Tarnai, 1999) and is adopted here for the vibration analysis. The structure is characterized by two stiffnesses denoted by D_1 and D_2, such that if we set either one of the stiffnesses equal to zero the structure would become a mechanism and consequently would not be capable to carry any load. According to Föppl's theorem the circular frequency of such a structure is approximated by $1/\omega^2 = 1/\omega_1^2 + 1/\omega_2^2$, where ω_1 is the circular frequency of the structure if D_2 is set equal to infinity, while ω_2 is the circular frequency if D_1 is set equal to infinity.

The above three approximations give the exact circular frequencies when the two eigenmodes, which belong to the circular frequencies ω_1 and ω_2, are identical.

As it was stated before we solved the differential equation of the continuum analytically and also with the aid of the above theorems. In Section 5 and 6 we define the error of the approximation as

$$\text{Er} = \frac{A_{\text{app}} - A_{\text{cont}}}{A_{\text{cont}}}, \tag{1}$$

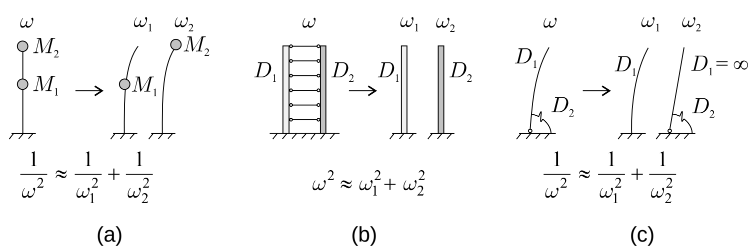

Fig. 2. Illustration of Dunkerley's (a), Southwell's (b) and Föppl's (c) theorems.

where "cont" refers to the exact solution of the continuum while "app" refers to the approximate solution, and A can be e.g. the circular frequency, the base shear force etc.

The total error of the suggested method comes from three sources (i) each lateral load-resisting subsystem is replaced by a continuous cantilever beam, (ii) these beams are then replaced by a single replacement beam, and (iii) the characteristics of the replacement beams are calculated approximately.

In Appendix A we verify the approximate method by solving structures with the aid of a FE method (ETABS) and by our approximate calculation. The error is defined as

$$\mathrm{Er} = \frac{A_{\mathrm{app}} - A_{\mathrm{ETABS}}}{A_{\mathrm{ETABS}}}, \tag{2}$$

where "ETABS" refers to the FE program ETABS.

4. Replacement beam

One of the most widely used approximate calculations is based on the "continuum method" (Hegedűs and Kollár, 1999; Skattum, 1971; Stafford Smith and Coull, 1991; Zalka, 2000), when the stiffened building structure is replaced by a (continuous) beam. The most general continuum model of a single lateral load-resisting subsystem is a sandwich beam (Hegedűs and Kollár, 1999), shown in Fig. 3. A sandwich beam is characterized by three different stiffnesses: the global bending stiffness, D_0, the local bending stiffness, D_l and the shear stiffness, S (Fig. 3). The calculation of the replacement stiffnesses of different lateral load-resisting subsystems are given in the literature (Beck, 1962; Hegedűs and Kollár, 1999; Köpecsiri, 1997; Szerémi, 1978; Zalka, 2000), the general cases are summarized in Potzta and Kollár (2003).

When a symmetrical structure consists of several lateral load-resisting subsystems, the stiffnesses of the beam which replaces the whole bracing system are (Potzta and Kollár, 2003):

$$S = \pi^2 \frac{B^3}{C^2}, \quad D_0 = \frac{1}{\frac{C}{B^2} - \frac{1}{l_0^2}\frac{C^2}{B^3}}, \quad D_l = A - \frac{B^2}{C}, \tag{3}$$

where

$$A = \sum_{k=1}^{n} \left(\frac{D_{0k}}{1 + \frac{\pi^2 D_{0k}}{l_0^2 S_k}} + D_{lk} \right),$$
$$B = \sum_{k=1}^{n} \frac{D_{0k}}{\left(1 + \frac{\pi^2 D_{0k}}{l_0^2 S_k}\right)^2} \frac{\pi^2 D_{0k}}{S_k}, \tag{4}$$
$$C = \sum_{k=1}^{n} \frac{D_{0k}}{\left(1 + \frac{\pi^2 D_{0k}}{l_0^2 S_k}\right)^3} \left(\frac{\pi^2 D_{0k}}{S_k}\right)^2.$$

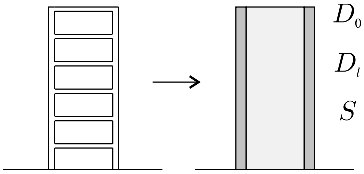

Fig. 3. Replacement sandwich beam.

D_{0k}, D_{lk}, and S_k represents the stiffnesses of the kth lateral load-resisting subsystem, l_0 depends on the variation of the lateral load (Potzta and Kollár, 2003). In vibration analysis we suggest the following approximate value of l_0: $l_0 = 2H$ for the calculations in the first mode, $l_0 = \frac{2}{3}H$ for the calculations in the second mode, and $l_0 = \frac{2}{5}H$ for third mode of vibration.

An unsymmetrical structure develops coupled lateral–torsional vibration. In the analysis of spatial vibration problem the behavior of the lateral load-resisting subsystems is described by the following stiffness matrices:

$$[D_l] = \begin{bmatrix} D_{lzz} & D_{lzy} & D_{lz\omega} \\ D_{lyz} & D_{lyy} & D_{ly\omega} \\ D_{l\omega z} & D_{l\omega y} & D_{l\omega\omega} \end{bmatrix}, \quad [D_0] = \begin{bmatrix} D_{0zz} & D_{0zy} & D_{0z\omega} \\ D_{0yz} & D_{0yy} & D_{0y\omega} \\ D_{0\omega z} & D_{0\omega y} & D_{0\omega\omega} \end{bmatrix}, \quad [S] = \begin{bmatrix} S_{yy} & S_{yz} & S_{y\omega} \\ S_{zy} & S_{zz} & S_{z\omega} \\ S_{\omega z} & S_{\omega y} & S_{\omega\omega} \end{bmatrix}. \tag{5}$$

The calculation of elements of the stiffness matrices are given in the literature (Kollár, 2001; Potzta, 2002).

For the vibration analysis of an unsymmetrical structure (consisting of an arbitrary combination of lateral load-resisting subsystems) the replacement stiffness matrices should be calculated as follows (Potzta and Kollár, 2003):

$$\begin{aligned} [S] &= \pi^2 [B][C]^{-1}[B][C]^{-1}[B], \\ [D_0] &= [B][C]^{-1}[B]\left[[E] - \frac{1}{l_0^2}[B]^{-1}[C]\right]^{-1}, \\ [D_l] &= [A] - [B][C]^{-1}[B], \\ D_t &= \sum_{k=1}^{n} D_{tk}, \end{aligned} \tag{6}$$

where

$$\begin{aligned} A &= \sum_{k=1}^{n} \left(\left([E] + \frac{\pi^2}{l_0^2}[D_0]_k [S]_k^{-1} \right)^{-1} [D_0]_k + [D_l]_k \right), \\ B &= \sum_{k=1}^{n} \pi^2 \left([E] + \frac{\pi^2}{l_0^2}[D_0]_k [S]_k^{-1} \right)^{-1} [D_0]_k [S]_k^{-1} \left([E] + \frac{\pi^2}{l_0^2}[D_0]_k [S]_k^{-1} \right)^{-1} [D_0]_k, \\ C &= \sum_{k=1}^{n} \pi^4 \left([E] + \frac{\pi^2}{l_0^2}[D_0]_k [S]_k^{-1} \right)^{-1} [D_0]_k [S]_k^{-1} \left([E] + \frac{\pi^2}{l_0^2}[D_0]_k [S]_k^{-1} \right)^{-1} \\ &\quad \times [D_0]_k [S]_k^{-1} \left([E] + \frac{\pi^2}{l_0^2}[D_0]_k [S]_k^{-1} \right)^{-1} [D_0]_k. \end{aligned} \tag{7}$$

$[D_0]_k$, $[D_l]_k$, and $[S]_k$ are the stiffness matrices of the kth lateral load-resisting subsystem, l_0 has the same values as in the lateral analysis.

5. Circular frequency and period of vibration

In this section simple formulas are developed for the calculation of the circular frequencies of replacement sandwich beams. We recall that the circular frequency, ω is related to the period of vibration, T and to the frequency, f by

$$T = \frac{2\pi}{\omega}, \quad f = \frac{\omega}{2\pi}. \tag{8}$$

5.1. Uniform mass distribution along the height

5.1.1. Plane problem

We consider a building structure with a symmetrical plan which vibrates in the x–z symmetry plane. The stiffnesses of the replacement beam in the x–z plane are the shear stiffness (S), the global bending stiffness (D_0) and the local bending stiffness (D_l). The circular frequencies of beams which undergo bending or shear deformations only are summarized in Table 2 (Köpecsiri, 1997).

The circular frequency of a sandwich beam with constant mass distribution was determined in Köpecsiri (1997). An approximate expression can be obtained by using Föppl's and Southwell's theorems (Köpecsiri, 1997):

$$\omega_{mi}^2 = \left(\frac{1}{(\omega_{mi}^{B_0})^2} + \frac{1}{(\omega_{mi}^{S})^2} \right)^{-1} + (\omega_{mi}^{B_l})^2 \quad i = 1, 2, \ldots, \tag{9}$$

where $i = 1$ belongs to the first mode of vibration, $\omega_{mi}^{B_0}$ and $\omega_{mi}^{B_l}$ are the circular frequencies of beams with bending stiffnesses D_0 and D_l, respectively; and ω_{mi}^{S} is the circular frequency of a beam which undergoes shear deformation only and whose shear stiffness is S. From the second row of Table 2 we have

Table 2
Circular frequencies of beams capable bending deformations only or shear deformations only

Mass and boundary conditions	Bending deformation only	Shear deformation only
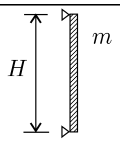	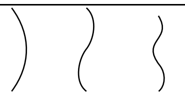 $i=1 \quad i=2 \quad i=3$ $\omega_{Bi} = \mu_{Bi}\sqrt{\frac{D}{mH^4}}$ $\mu_{B1} = \pi$ $\mu_{B2} = 2\pi$ $\mu_{B3} = 3\pi$	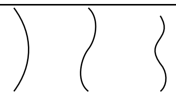 $i=1 \quad i=2 \quad i=3$ $\omega_{Si} = \mu_{\mathrm{Si}}\sqrt{\frac{S}{mH^2}}$ $\mu_{S1} = \pi$ $\mu_{S2} = 2\pi$ $\mu_{S^3} = 3\pi$
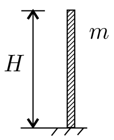	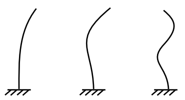 $i=1 \quad i=2 \quad i=3$ $\omega_{Bi} = \mu_{Bi}\sqrt{\frac{D}{mH^4}}$ $\mu_{B1} = 3.52$ $\mu_{B2} = 22.03$ $\mu_{B3} = 61.7$	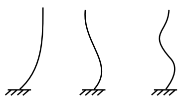 $i=1 \quad i=2 \quad i=3$ $\omega_{Si} = \mu_{\mathrm{Si}}\sqrt{\frac{S}{mH^2}}$ $\mu_{S1} = 0.5\pi$ $\mu_{S2} = 1.5\pi$ $\mu_{S3} = 2.5\pi$
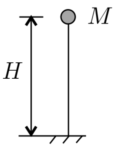	 $\omega_B = \sqrt{3}\sqrt{\frac{D}{MH^3}}$	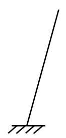 $\omega_S = \sqrt{\frac{S}{MH}}$

$$\omega_{mi}^{B_0} = \mu_{Bi}\sqrt{\frac{D_0}{mH^4}}, \quad \omega_{mi}^{B_1} = \mu_{Bi}\sqrt{\frac{D_1}{mH^4}}, \quad \omega_{mi}^{S} = \mu_{Si}\sqrt{\frac{S}{mH^2}}, \tag{10}$$

where m is the mass per unit height.

Numerical comparisons with the exact solution for the circular frequencies shows that for $i = 1$ Eq. (9) may underestimate the circular frequency by up to 16% ($-16\% \leqslant \mathrm{Er} \leqslant 0$) for $i = 2$ may underestimate the circular frequency by up to 11% and overestimate it by up to 9% ($-11\% \leqslant \mathrm{Er} \leqslant 9\%$), while for $i = 3$ may underestimate the circular frequency by up to 4% and overestimate it by up to 6% ($-4\% \leqslant \mathrm{Er} \leqslant 6\%$).

The accuracy of this approximation is suitable for design purposes. However, in some special cases the designer would need more accurate results, thus we suggest a correction factor to reduce the errors of Eq. (9). We derived an approximate formula in the function of the stiffness ratios $\alpha = H\sqrt{\frac{S}{D_1}}$ and $\beta = \sqrt{\frac{D_1}{D_0}}$:

$$\omega_{m1}^2 = \left[\left(\frac{1}{(\omega_{m1}^{B_0})^2} + \frac{1}{(\omega_{m1}^{S})^2}\right)^{-1} + (\omega_{m1}^{B_1})^2\right] \Big/ (1 - f), \tag{11}$$

where

$$f = \frac{2}{100(1 + 2.7\beta)}\left(\frac{1.1}{1.1 + \mathrm{e}^{-1.6\xi} - \mathrm{e}^{-0.0125\xi}} - 1\right), \quad \xi = \alpha(1 + 4\beta). \tag{12}$$

Eq. (11) may overestimate and underestimate the lowest circular frequency by up to 2.3% ($-2.3\% \leqslant \mathrm{Er} \leqslant 2.3\%$).

5.1.2. Spatial problem

The replacement beam of the stiffening system has the following stiffnesses (Potzta and Kollár, 2003):

$$[D_0] = \begin{bmatrix} D_{0zz} & D_{0zy} & D_{0z\omega} \\ D_{0yz} & D_{0yy} & D_{0y\omega} \\ D_{0\omega z} & D_{0\omega y} & D_{0\omega\omega} \end{bmatrix}, \quad [D_l] = \begin{bmatrix} D_{lzz} & D_{lzy} & D_{lz\omega} \\ D_{lyz} & D_{lyy} & D_{ly\omega} \\ D_{l\omega z} & D_{l\omega y} & D_{l\omega\omega} \end{bmatrix}$$
$$[S] = \begin{bmatrix} S_{yy} & S_{yz} & S_{y\omega} \\ S_{zy} & S_{zz} & S_{z\omega} \\ S_{\omega z} & S_{\omega y} & S_{\omega\omega} \end{bmatrix}, \quad D_t, \tag{13}$$

where $[D_0]$ and $[D_l]$ are the matrices of the global and local bending stiffnesses, respectively, $[S]$ is the shear stiffness matrix and D_t is the torsional stiffness. The calculation of the elements of $[D_0]$, $[D_l]$, and $[S]$ are given in Section 4. (We note that the axis of the replacement beam passes through the centroid of the coordinate system which may be chosen arbitrarily.)

The circular frequencies for beams where both ends are *simply supported* and $[D_l]$ is zero were derived in Kollár (2001). Following the same steps as in Kollár (2001) but taking also $[D_l]$ into account, we obtain the following eigenvalue problem for the circular frequency, ω_{mi} (see Eq. (13) in Kollár (2001))

$$\left[\left(\frac{H^4}{\mu_{Bi}^2}[D_0]^{-1} + \frac{H^2}{\mu_{Si}^2}[S]^{-1}\right)^{-1} + \frac{\mu_{Bi}^2}{H^4}[D_l] + \frac{\mu_{Si}^2}{H^2}[G] - \omega_{mi}^2 m[M]\right]\begin{Bmatrix} v_{0m} \\ w_{0m} \\ \psi_{0m} \end{Bmatrix} = 0, \tag{14}$$

where for simply supported beams μ_{Bi} and μ_{Si} are given in the first row of Table 2; m is the mass per unit height, matrices $[M]$ and $[G]$ are

$$[M] = \begin{bmatrix} 1 & 0 & z_m \\ 0 & 1 & -y_m \\ z_m & -y_m & \frac{\Theta}{m} + y_m^2 + z_m^2 \end{bmatrix}, \quad [G] = \begin{bmatrix} 0 & 0 & 0 \\ 0 & 0 & 0 \\ 0 & 0 & D_t \end{bmatrix}, \tag{15}$$

Θ is the polar moment of mass (per unit height) about the mass center, and y_m, z_m are the coordinates of the mass center. The eigenvector of Eq. (14) contains the amplitudes of vibration in the *x–z* plane (w_{0m}), *x–y* plane (v_{0m}) and the amplitude of the torsional mode (ψ_{0m}).

For a *cantilever beam*, we adopt Eq. (14) as an approximation, but we introduce values for μ_{Bi} and μ_{Si} given in the second row of Table 2. We obtain three circular frequencies (and three corresponding eigenvectors) for each value of *i*. The accuracy of Eq. (14) was also investigated numerically. We obtained the same accuracy for ω as for the plane problem.

Doubly symmetrical building. When both the *x–z* and the *x–y* planes are symmetry planes, the building vibrates either in the *x–z* plane, or in the *x–y* plane, or torsionally about the *x*-axis. In this case the off-diagonal elements of matrices $[D_0]$, $[D_1]$, and $[S]$ are zero, and, accordingly, Eq. (14) gives the following three sets of circular frequencies:

$$\begin{aligned}
\omega_{ymi}^2 &= \left(\frac{1}{\mu_{Bi}^2 \frac{D_{0zz}}{mH^4}} + \frac{1}{\mu_{Si}^2 \frac{S_{yy}}{mH^2}} \right)^{-1} + \mu_{Bi}^2 \frac{D_{1yy}}{mH^4}, \quad \text{vibration in the } x\text{–}y \text{ plane}, \\
\omega_{zmi}^2 &= \left(\frac{1}{\mu_{Bi}^2 \frac{D_{0yy}}{mH^4}} + \frac{1}{\mu_{Si}^2 \frac{S_{zz}}{mH^2}} \right)^{-1} + \mu_{Bi}^2 \frac{D_{1zz}}{mH^4}, \quad \text{vibration in the } x\text{–}z \text{ plane}, \\
\omega_{\omega mi}^2 &= \left(\frac{1}{\mu_{Bi}^2 \frac{D_{0\omega\omega}}{\Theta H^4}} + \frac{1}{\mu_{Si}^2 \frac{S_{\omega\omega}}{\Theta H^2}} \right)^{-1} + \mu_{Bi}^2 \frac{D_{1\omega\omega}}{\Theta H^4} + \mu_{Si}^2 \frac{GI_t}{\Theta H^2}, \quad \text{torsional vibration.}
\end{aligned} \tag{16}$$

We observe that the expression for ω_{zmi}^2 is identical to Eq. (9) developed for the plane problem.

Doubly symmetrical building with unsymmetrical mass. When the building is symmetrical with respect to both the *x–z* and the *x–y* planes, however the mass is not symmetrical with respect to these planes, Eq. (14) simplifies to

$$\left\{ \begin{bmatrix} \omega_{ymi}^2 & & \\ & \omega_{zmi}^2 & \\ & & \frac{\Theta}{m}\omega_{\omega mi}^2 \end{bmatrix} - \omega_{mi}^2 [M] \right\} \begin{Bmatrix} v_{0m} \\ w_{0m} \\ \psi_{0m} \end{Bmatrix} = 0, \tag{17}$$

where $[M]$ is defined by Eq. (15) and ω_{ymi}, ω_{zmi}, and $\omega_{\omega mi}$ are given in Eq. (16).

5.2. Additional mass at the top

5.2.1. Plane problem

When there is an additional mass (M) at the end of the cantilever (Fig. 4), the lowest circular frequency may be approximated by using Dunkerley's theorem as

$$\omega^2 = \left(\frac{1}{\omega_{m1}^2} + \frac{1}{\omega_M^2} \right)^{-1}, \tag{18}$$

where

$$\omega_M^2 \simeq \left(\frac{1}{(\omega_M^{B_0})^2} + \frac{1}{(\omega_M^S)^2} \right)^{-1} + (\omega_M^{B_1})^2 \tag{19}$$

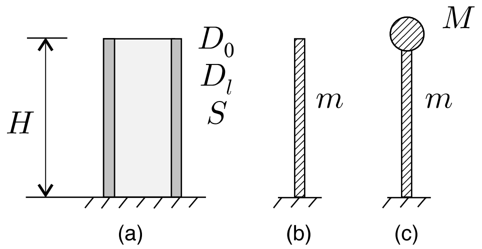

Fig. 4. Sandwich beam (a); constant mass distribution (b); constant mass and additional mass at the top (c).

and (see Table 2, third row)

$$\omega_M^{B_0} = \sqrt{3}\sqrt{\frac{D_0}{MH^3}}, \quad \omega_M^{B_1} = \sqrt{3}\sqrt{\frac{D_1}{MH^3}}, \quad \omega_M^S = \sqrt{\frac{S}{MH}}. \tag{20}$$

The accuracy of Eq. (19) was found to be $-6\% \leqslant \mathrm{Er} \leqslant 0$.

5.2.2. Spatial problem

In case of spatial vibration the circular frequencies belonging to $i = 1$ can be calculated as (see Dunkerley's theorem)

$$\omega^2 = \left(\frac{1}{\omega_{m1}^2} + \frac{1}{\omega_M^2}\right)^{-1}, \tag{21}$$

where ω_M is calculated from the following equation (Potzta and Kollár, 2003):

$$\left[\left(\frac{H^3}{3}[D_0]^{-1} + H[S]^{-1}\right)^{-1} + \frac{3}{H^3}[D_l] + \frac{1}{H}[G] - \omega_{mi}^2 M[\Omega]\right]\begin{Bmatrix} v_{0M} \\ w_{0M} \\ \psi_{0M}\end{Bmatrix} = 0, \tag{22}$$

where M is the additional mass at the top and matrix $[\Omega]$ is given by

$$[\Omega] = \begin{bmatrix} 1 & 0 & z_M \\ 0 & 1 & -y_M \\ z_M & -y_M & \frac{\Theta}{M} + y_M^2 + z_M^2 \end{bmatrix}, \tag{23}$$

where Θ is the polar moment of mass (at the top) about the mass center, and y_M, z_M are the coordinates of the mass center.

Care must be taken in the use of Eq. (21). Eq. (21) may give unacceptable error when the horizontal distribution of masses at the top is significantly different from the mass distribution on the other floors. In this case the eigenvectors for the uniform mass distribution and those for the mass on the top are very different. Hence, the use of Eq. (21) is recommended only if the scalar product of the eigenvectors are close to unity, say $v_{0M}v_{om} + w_{0M}w_{0m} + \psi_{0M}\psi_{0m} > 0.9$.

6. Internal forces

In the response modal analysis of buildings subjected to earthquakes an equivalent load is determined in each mode of vibration. For in-plane vibration, when the ground motion is in the plane of the vibration, the horizontal force is (Chopra, 1995)

$$f_i(x) = \frac{\int_0^H m\phi_i(x)\,\mathrm{d}x}{\int_0^H m\phi_i^2(x)\,\mathrm{d}x} m\phi_i(x) S_{Ai}, \tag{24}$$

where S_{Ai} is the spectral acceleration (which depends on the period of vibration, damping and the ground peak acceleration), and ϕ_i is the mode shape.

For spatial vibration (Chopra, 1995)

$$\{f\}_i = \begin{Bmatrix} f_{yi} \\ f_{zi} \\ f_{\omega i} \end{Bmatrix} = \frac{\int_0^H \{\phi_i(x)\}^{\mathrm{T}}[M]\,\mathrm{d}x\{\imath\}}{\int_0^H \{\phi_i(x)\}^{\mathrm{T}}[M]\{\phi_i(x)\}\,\mathrm{d}x} m[M] \begin{Bmatrix} \phi_{yi}(x) \\ \phi_{zi}(x) \\ \phi_{\Theta ni}(x) \end{Bmatrix} S_{Ai}, \tag{25}$$

where f_{yi} and f_{zi} are horizontal forces in the y and z directions, respectively, $f_{\omega i}$ is the resultant moment about the x-axis, and $\{\imath\}$ is the influence vector (Chopra, 1995), which represents the direction of excitation. For example if the excitation is in the x–y plane $\{\imath\} = \{1, 0, 0\}$, if the excitation is in the x–η plane (where η is in the y–z plane, and the angle between y and η is ϑ) $\{\imath\} = \{\cos\vartheta, \sin\vartheta, 0\}$, and for torsional excitation $\{\imath\} = \{0, 0, 1\}$.

6.1. Uniform mass distribution along the height

6.1.1. Plane problem

In this section we consider symmetrical structures subjected to earthquakes in the symmetry plane.

Base shear force. The total horizontal load, which is identical to the base shear force, is obtained by integrating Eq. (24) over the height of the building.

For uniform mass distribution, integration of Eq. (24) gives

$$V_i = \int_0^H f_i(x)\,\mathrm{d}x = \frac{\left(\int_0^H \phi_i(x)\,\mathrm{d}x\right)^2}{\int_0^H \phi_i^2(x)\,\mathrm{d}x} m S_{Ai} = v_i m H S_{Ai}, \tag{26}$$

the values of the multiplier, v_i are given in Table 3 for the first, second and third periods of vibration for beams undergo bending deformation ($v_i = v_{B1}$, $v_i = v_{B2}$, $v_i = v_{B3}$) and for beams undergo shear deformation only ($v_i = v_{S1}$, $v_i = v_{S2}$, $v_i = v_{S3}$).

For a sandwich beam, the multiplier lies between these two values i.e. for the first period of vibration $0.61 < v_i < 0.81$, and for the second period of vibration $0.09 < v_i < 0.188$ and for the third $0.032 < v_i < 0.065$. To estimate v_i for a sandwich beam we adopt the approximate formula of the circular frequency. Eqs. (9) and (10) gives

Table 3
The values of the multiplier, v_i for the calculation of the internal forces

Mode	Deformation	Base shear force	Shear force at $3/4H$	Base overturning moment
1	Bending deformation only (v_{B1})	0.61	0.32	0.45
	Shear deformation only (v_{S1})	0.81	0.32	0.52
2	Bending deformation only (v_{B2})	0.188	0.09	0.039
	Shear deformation only (v_{S2})	0.09	0.09	0.018
3	Bending deformation only (v_{B3})	0.065	0.033	0.00825
	Shear deformation only (v_{S3})	0.032	0.033	0.0044

$$1 = \left(\left(\frac{1}{\mu_{Bi}^2 \frac{D_0}{mH^4}} + \frac{1}{\mu_{Si}^2 \frac{S}{mH^2}} \right)^{-1} + \mu_{Bi}^2 \frac{D_l}{mH^4} \right)^{-1} \omega_{mi}^2. \tag{27}$$

The value of v_i is approximated as

$$v_i = \left(\left(\frac{v_{Bi}}{\mu_{Bi}^2 \frac{D_0}{mH^4}} + \frac{v_{Si}}{\mu_{Si}^2 \frac{S}{mH^2}} \right)^{-1} + \frac{1}{v_{Bi}} \mu_{Bi}^2 \frac{D_l}{mH^4} \right)^{-1} \omega_{mi}^2, \tag{28}$$

where v_{Bi} and v_{Si} are given in Table 3. This expression gives the exact value for v_i when $S \to \infty$, or $S \to 0$, or $D_0 \to 0$, or $D_0 \to \infty$ and $D_l \to 0$. For arbitrary values of D_0, D_l and S Eq. (28) was verified numerically. Comparisons with the exact solution of Eq. (26) for a sandwich beam showed that the accuracy of Eq. (28) for v_1 is $-9\% < \text{Er} < 0$, for v_2 is $-37\% < \text{Er} < 0$, while for v_3 is $-27\% < \text{Er} < 0$.

Shear force at height $3/4H$. The distribution of the horizontal forces is determined by the mode shape of the beam (see Eq. (24)). In the first, second, and third modes of vibration the mode shape, the distribution of horizontal seismic forces and the shear forces along the height are illustrated in Fig. 5. The maximum of the shear force arises at the bottom of the cantilever, but in the second mode there is another local maximum (Fig. 5, middle).

This local maximum for different continuum models and different stiffness distributions was calculated, and the location of the maximum was found to be between $0.6H$ and $0.9H$. The maximum can be approximated by evaluating the shear force at height $3/4H$

$$V_i^{3/4} = v_i mHS_{Ai}. \tag{29}$$

The constant for beams with bending deformation or shear deformation only is given in Table 3 (column "shear force at $3/4H$"), for the first three modes. For a sandwich beam Eq. (29) $v_i = v_{Bi} = v_{Si}$ can be used.

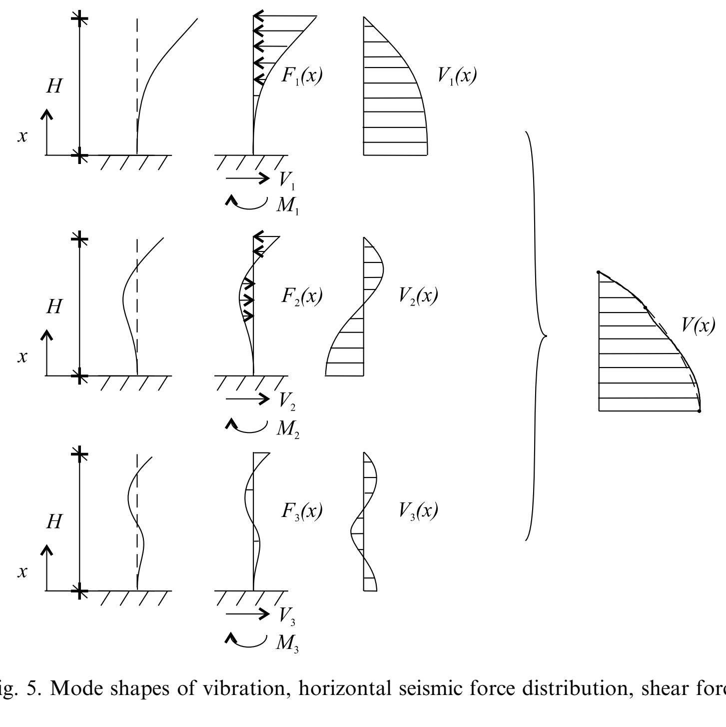

Fig. 5. Mode shapes of vibration, horizontal seismic force distribution, shear force.

The maximum error of this approximation for v_1 is $-3\% < \mathrm{Er} < +3\%$, for v_2 is $-2\% < \mathrm{Er} < 10\%$, while for v_3 is $-7\% < \mathrm{Er} < +4\%$.

(The design value of the shear force can be calculated by combining the modal responses. There are different combination rules given in design codes. We suggest to calculate the design value of shear force at the bottom of the cantilever and at height $3/4H$. At the top of the cantilever the shear force is zero. The shear force diagram may be approximated by fitting a second order parabola to the design value of the shear force at these three point. See Fig. 5.)

Base overturning moment. The base overturning moment can be calculated from the horizontal load Eq. (24) as follows.

For a uniform mass distribution we have

$$M_i = \int_0^H x f_i(x)\,\mathrm{d}x = \frac{\int_0^H \phi_i(x)\,\mathrm{d}x \int_0^H x\phi_i(x)\,\mathrm{d}x}{\int_0^H \phi_i^2(x)\,\mathrm{d}x} m S_{Ai} = v_i m H^2 S_{Ai}. \tag{30}$$

The multiplier v_i is given in Table 3 for a beam undergoes bending deformation and for a beam undergoes shear deformation only. For a sandwich beam the multiplier lies between these two values. v_i is again calculated from Eq. (28) by introducing the values of v_i given in the last column of Table 3. Numerical comparisons showed that Eq. (28) gives the value of v_1 with an error $-5\% < \mathrm{Er} < 1\%$, while for the second and third modes the results are not acceptable.

6.1.2. Spatial problem

Base shear force. The base shear forces and the resultant torque (Fig. 6) can be calculated from the integration of Eq. (25).

$$\begin{Bmatrix} V_{yi} \\ V_{zi} \\ V_{\omega i} \end{Bmatrix} = \int_0^H \begin{Bmatrix} f_{yi} \\ f_{zi} \\ f_{\omega i} \end{Bmatrix} \mathrm{d}x. \tag{31}$$

First we consider the case when the structure consists of lateral load-resisting subsystems which undergo shear deformation only. In this case the functions in the eigenvector (ϕ_{yi}, ϕ_{zi}, $\phi_{\omega i}$) are cosines and Eqs. (25) and (31) give

$$\begin{Bmatrix} V_{yi} \\ V_{zi} \\ V_{\omega i} \end{Bmatrix} = \frac{\{\phi_{0i}\}^{\mathrm{T}}[M]\{\imath\}}{\{\phi_{0i}\}^{\mathrm{T}}[M]\{\phi_{0i}\}} m[M]H v_i \{\phi_{0i}\} S_{Ai}, \tag{32}$$

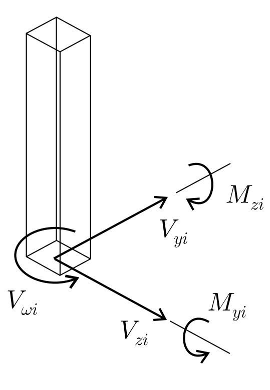

Fig. 6. The base shear forces (V_{yi}, V_{zi}), the resultant torque ($V_{\omega i}$), and the base overturning moments (M_{yi}, M_{zi}).

where $\{\phi_{0i}\}$ is the eigenvector of Eq. (14)

$$\{\phi_{0i}\} = \begin{Bmatrix} v_{0mi} \\ w_{0mi} \\ \psi_{0mi} \end{Bmatrix}, \tag{33}$$

and (for $i = 1$) $v_i = v_{Si} = 0.81$ (Table 3). The same equation applies when the lateral load-resisting subsystems have bending deformation only, but we must substitute $v_i = v_{Bi} = 0.61$ into Eq. (32).

When the lateral load-resisting subsystems are sandwiches, the horizontal forces can be calculated by

$$\begin{Bmatrix} V_{yi} \\ V_{zi} \\ V_{\omega i} \end{Bmatrix} = \frac{\{\phi_0\}^{\mathrm{T}}[M]\{\imath\}}{\{\phi_0\}^{\mathrm{T}}[M]\{\phi_0\}} m[M]H \begin{Bmatrix} v_{yi}v_{0mi} \\ v_{zi}w_{0mi} \\ v_{\omega i}\psi_{0mi} \end{Bmatrix} S_{Ai}, \tag{34}$$

where v_{yi}, v_{zi}, and $v_{\omega i}$ are multipliers with values between v_{Bi} and v_{Si} (i.e. for $i = 1$, $0.61 < v_1 < 0.81$ and for $i = 2$, $0.09 < v_2 < 0.188$), see Table 3. To obtain a reasonable estimation for v, we rearrange the expression obtained for the circular frequencies. By multiplication of Eq. (14) by $[M]^{-1}/m\omega_{mi}^2$ we obtain

$$\begin{Bmatrix} v_{0mi} \\ w_{0mi} \\ \psi_{0mi} \end{Bmatrix} = \left[\left(\frac{H^4}{\mu_{Bi}^2}[D_0]^{-1}[M] + \frac{H^2}{\mu_{Si}^2}[S]^{-1}[M] \right)^{-1} + \frac{\mu_{Bi}^2}{H^4}[M]^{-1}[D_1] + \frac{\mu_{Si}^2}{H^2}[M]^{-1}[G] \right]^{-1} \begin{Bmatrix} v_{0mi} \\ w_{0mi} \\ \psi_{0mi} \end{Bmatrix} \omega_{mi}^2 m. \tag{35}$$

Similarly as it was done for the plane problem (see Eq. (28)) we introduce vs into this equation and obtain

$$\begin{Bmatrix} v_{yi}v_{0m} \\ v_{zi}w_{0m} \\ v_{\omega i}\psi_{0m} \end{Bmatrix} = \left[\left(\frac{v_{Bi}H^4}{\mu_{Bi}^2}[D_0]^{-1}[M] + \frac{v_{Si}H^2}{\mu_{Si}^2}[S]^{-1}[M] \right)^{-1} + \frac{\mu_{Bi}^2}{v_{Bi}H^4}[M]^{-1}[D_1] + \frac{\mu_{Si}^2}{v_{Si}H^2}[M]^{-1}[G] \right]^{-1} \times \begin{Bmatrix} v_{0mi} \\ w_{0mi} \\ \psi_{0mi} \end{Bmatrix} \omega_{mi}^2 m, \tag{36}$$

which is an approximate expression for the vector $\{v_{yi}v_{0mi}, v_{zi}w_{0mi}, v_{\omega i}\psi_{0mi}\}^{\mathrm{T}}$. With this approximation Eq. (34) can be directly evaluated for the seismic loads.

(Note that Eqs. (34) and (36) give the "exact" values of the horizontal forces (V_{yi} and V_{zi}) and the resultant torque ($V_{\omega i}$) when the structure is doubly symmetrical and in one direction it has shear deformation only, in the other direction it has bending deformation only, and in torsion it has bending or shear deformation only.)

As a rule, Eqs. (34) and (36) give only approximate values of the forces and the resultant moment. The numerical examples showed that the accuracies are the same as for the plane problem.

Base overturning moment. The base overturning moments can be obtained in the same way as the base shear forces. (Note that we may use the approximation only for the first mode.)

From Eq. (25) we arrive at

$$\begin{Bmatrix} M_{z1} \\ M_{y1} \\ B_1 \end{Bmatrix} = \int_0^H x \begin{Bmatrix} f_{y1} \\ f_{z1} \\ f_{\omega 1} \end{Bmatrix} \mathrm{d}x = \frac{\{\phi_{01}\}^{\mathrm{T}}[M]\{\imath\}}{\{\phi_{01}\}^{\mathrm{T}}[M]\{\phi_{01}\}} m[M]H^2 \begin{Bmatrix} v_{y1}v_{0m1} \\ v_{z1}w_{0m1} \\ v_{\omega 1}\psi_{0m1} \end{Bmatrix} S_{A1}, \tag{37}$$

where M_{z1}, and M_{y1} are the base overturning moments in the x–y and x–z planes. The vector on the right hand side is approximated by Eq. (36) where $v_{B1} = 0.45$ and $v_{S1} = 0.52$ (see Table 3).

We may observe that when there is only bending deformation, $v_y = v_z = v_\omega = 0.45$, and when there is only shear deformation, $v_y = v_z = v_\omega = 0.52$.

6.2. Additional mass at the top

6.2.1. Plane problem

When there is an additional mass on the top, we have to take the following additional force and base overturning moment into account:

$$F_M = MS_A, \quad M_M = HMS_A.$$

6.2.2. Spatial problem

In case of spatial vibration when there are additional masses at the top, concentrated forces and moment about the x-axis may arise on the top of the building structure. The resultant forces (V_y^M and V_z^M) and moment (V_ω^M) are (Chopra, 1995)

$$\left\{ \begin{array}{c} V_y^M \\ V_z^M \\ V_\omega^M \end{array} \right\} = \frac{\{\phi_0\}^{\mathrm{T}}[M]\{\iota\}}{\{\phi_0\}^{\mathrm{T}}[M]\{\phi_0\}} M[\Omega]\{\phi_0\}S_A. \tag{38}$$

The additional base overturning moments have the values

$$M_z^M = HV_y^M, \quad M_y^M = HV_z^M.$$

7. Conclusion

We presented a simple approximate method for the calculation of the period of vibrations and base internal forces of building structures with identical stories subjected to earthquakes. We considered symmetrical and unsymmetrical building structures stiffened by shear walls, coupled shear walls, trusses, frames or cores. We solved the vibration problem in case of lateral, torsional and spatial lateral–torsional vibration.

The accuracy of the approximation was verified by two numerical examples.

Acknowledgements

The authors wish to thank professor Helmut Krawinkler (Stanford University) for his valuable suggestions. This work was supported by the Hungarian Science Foundation (OTKA, no T0 32053).

Appendix A. Numerical example

In this section two numerical examples are presented to demonstrate the accuracy and robustness of the approximate calculation.

A.1. Symmetrical building

First we consider a doubly symmetrical building shown in Fig 7. The building is stiffened in the y direction by solid walls while in the z direction by two solid walls at the symmetry plane and by two coupled shear walls arranged symmetrically. The geometric and material characteristics are given in Table 5.

The approximate calculation was carried out in the following steps:

Step 1. Calculation of the stiffnesses of the lateral load-resisting subsystems (Table 2).
Step 2. Calculation of the replacement stiffnesses of the building by Eqs. (3) and (4).
Step 3. Calculation the circular frequencies by Eq. (16).
Step 4. We will calculate the base shear force for an excitation in the x–z plane (Eqs. (26) and (28)).

The periods of vibration and the base shear forces were also determined by a FE code (ETABS). In the example uniform mass distribution was considered.

Step 1. The stiffnesses of the solid walls are (Table 2.)

$$D_0^{\mathrm{w}} = E^{\mathrm{wa}} I^{\mathrm{wa}} = 8.85 \times 10^7 \ \mathrm{kN\,m^2}, \quad D_1^{\mathrm{w}} = 0, \quad S^{\mathrm{w}} = \infty. \tag{A.1}$$

The stiffnesses of the coupled shear walls are

$$\begin{aligned} D_1^{\mathrm{c}} &= 2E^{\mathrm{w}} I^{\mathrm{wa}} = 1.77 \times 10^8 \ \mathrm{kN\,m^2}, \\ D_0^{\mathrm{c}} &= 2E^{\mathrm{w}} A^{\mathrm{wa}} (c^{\mathrm{w}})^2 = 1.37 \times 10^9 \ \mathrm{kN\,m^2}, \end{aligned} \tag{A.2}$$

$$S^{\mathrm{c}} = \left(\left(\frac{6E_{\mathrm{b}} I_{\mathrm{b}} 2(d+s_1)^2}{d^3 h \left(1 + \frac{12\rho E_{\mathrm{b}} I_{\mathrm{b}}}{G_{\mathrm{b}} d^2 A_{\mathrm{b}}}\right)} \right)^{-1} + \left(2\frac{12E^{\mathrm{w}} I^{\mathrm{wa}}}{h^2} \right)^{-1} \right)^{-1} = 9.99 \times 10^4 \ \mathrm{kN}.$$

Step 2. The stiffnesses in the y direction are identical to two times those given by Eq. (A.1). The stiffnesses in the z direction are calculated by Eqs. (3) and (4), and are (with $l = 2H = 166.4$ m)

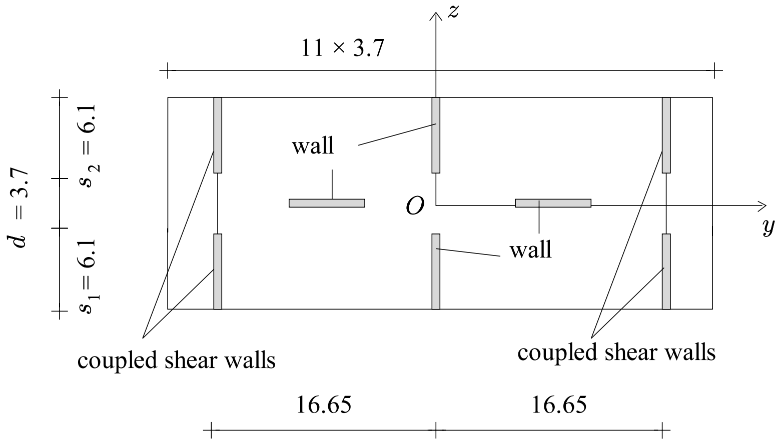

Fig. 7. Numerical example of Appendix A.1.

$$
\begin{aligned}
A &= 2\left(\frac{D_0^c}{1+\frac{\pi^2 D_0^c}{l_0^2 S^c}} + D_1^c\right) + 2D_0^w = 9.96\times 10^8\ \mathrm{kN\,m^2},\\
B &= 2\frac{D_0^c}{\left(1+\frac{\pi^2 D_0^c}{l_0^2 S^c}\right)^2}\frac{\pi^2 D_0^c}{S^c} = 1.07\times 10^{13}\ \mathrm{kN\,m^4},\\
C &= 2\frac{D_0^c}{\left(1+\frac{\pi^2 D_0^c}{l_0^2 S^c}\right)^3}\left(\frac{\pi^2 D_0^c}{S^c}\right)^2 = 2.45\times 10^{17}\ \mathrm{kN\,m^6},\\
D_{0zz} &= \frac{1}{\frac{C}{B^2}-\frac{1}{l_0^2}\frac{C^2}{B^3}} = 2.73\times 10^9\ \mathrm{kN\,m^2},\\
S_{zz} &= \pi^2\frac{B^3}{C^2} = 5.30\times 10^8\ \mathrm{kN},\\
D_{lzz} &= A - \frac{B^2}{C} = 2.01\times 10^5\ \mathrm{kN\,m^2}.
\end{aligned}
\tag{A.3}
$$

The torsional stiffnesses are (from Eq. (6) and (7))

$$
\begin{aligned}
&D_{l\omega\omega} = \frac{1}{2}r^2 D_1^c = 7.60\times 10^{11}\ \mathrm{kN\,m^4},\quad D_{0\omega\omega} = \frac{1}{2}r^2 D_0^c = 9.82\times 10^{10}\ \mathrm{kN\,m^4},\\
&S_{\omega\omega} = \frac{1}{2}r^2 S^c = 5.54\times 10^7\ \mathrm{kN\,m^4},\quad D_t = 0.
\end{aligned}
\tag{A.4}
$$

Step 3. The circular frequencies are calculated by Eq. (16) by substituting $\mu_{B1} = 3.52$, $\mu_{S1} = 0.5\pi$ (Table 2) which gives

$$
\omega_{ym1} = 0.4042\frac{1}{\mathrm{sec}},\quad \omega_{zm2} = 0.8487\frac{1}{\mathrm{sec}},\quad \omega_{\omega m3} = 0.9857\frac{1}{\mathrm{sec}}. \tag{A.5}
$$

Note that the ETABS code results in

$$
\omega_{ym1} = 0.3939\frac{1}{\mathrm{sec}},\quad \omega_{zm2} = 0.9125\frac{1}{\mathrm{sec}},\quad \omega_{\omega m3} = 1.080\frac{1}{\mathrm{sec}}, \tag{A.6}
$$

which are within 9% of the above values.

We may improve the accuracy of Eq. (A.5) by taking Eqs. (11) and (12) into account. These formulae give instead of Eq. (A.5) the following values:

$$
\omega_{ym1} = 0.4051\frac{1}{\mathrm{sec}},\quad \omega_{zm2} = 0.8734\frac{1}{\mathrm{sec}},\quad \omega_{\omega m3} = 1.017\frac{1}{\mathrm{sec}}, \tag{A.7}
$$

which is within 6% of the ETABS calculation.

Step 1. The seismic forces are determined using the Response Modal Analysis. The calculation was carried out according to Eurocode 8. The spectral accelerations are given in the function of the period of vibration, (Eurocode 8)

$$\begin{aligned}
&0 < T_i < T_B \quad S_{ei} = a_g S_t \left[1 + \frac{T_i(\eta\beta - 1)}{T_B}\right],\\
&T_B < T_i < T_C \quad S_{ei} = a_g S_t \eta\beta,\\
&T_C < T_i < T_D \quad S_{ei} = a_g S_t \eta\beta \left(\frac{T_C}{T_i}\right)^{k_1},\\
&T_D < T_i \quad S_{ei} = a_g S_t \eta\beta \left(\frac{T_C}{T_D}\right)^{k_1} \left(\frac{T_D}{T_i}\right)^{k_2}.
\end{aligned} \tag{A.8}$$

The parameters in Eq. (A.8) depend on the soil condition, on the location of the structure, and on the damping ratio. We considered $S_t = 1$, $a_g = 0.08 \times 9.81$, $\beta = 2.5$, $T_B = 0.15$, $T_C = 0.6$, $T_D = 3$, $k_1 = 1$, $k_2 = 2$, $\eta = 1.323$.

Substituting the periods of vibration $T_i = 2\pi/\omega_{mi}$ (ω_{mi} is given by Eq. (A.5)) into Eq. (A.8) the spectral accelerations, S_{ei} can be determined in each mode of vibration. Base shear force in the *x–z* plane arise only in the second mode, and it is calculated by Eqs. (26) and (28) which yields

$$\begin{aligned}
&S_{e2} = 0.085,\\
&v_2 = \left(\left(\frac{v_{B1}}{\mu_{B1}^2 \frac{D_0}{mH^4}} + \frac{v_{S1}}{\mu_{S1}^2 \frac{S}{mH^2}}\right)^{-1} + \frac{1}{v_{B1}} \mu_{B1}^2 \frac{D_1}{mH^4}\right)^{-1} \omega_{mi}^2 = 0.6585,\\
&V_{z2} = v_2 mHS_{A2} = 1310.3 \text{ kN}.
\end{aligned} \tag{A.9}$$

The ETABS code results in $V_{z2} = 1481.45$ kN, which is within −12%.

Next we consider the same building, but we assume that the masses are offset by 5% in the *y* direction (this is recommended by Eurocode 8). As a consequence, we have $y_M = 2.035$ m, ($z_M = 0$), and the circular frequency can be determined from Eq. (17). The first line gives $\omega_{m1} = 0.4042$, while the second and third results in

$$\omega_{mi}^4 - \omega_{mi}^2 \left(\omega_{\omega mi}^2 + \omega_{zmi}^2 + \frac{m}{\Theta} \omega_{zmi}^2 y_M^2\right) + \omega_{\omega mi}^2 \omega_{zmi}^2 = 0. \tag{A.10}$$

From Eq. (A.10) the circular frequencies in the second and third mode can be calculated, and are

$$\omega_{m2} = 0.8229 \frac{1}{\text{sec}}, \quad \omega_{m3} = 1.016 \frac{1}{\text{sec}}. \tag{A.11}$$

The ETABS code results in

$$\omega_{m2} = 0.8874 \frac{1}{\text{sec}}, \quad \omega_{m3} = 1.1108 \frac{1}{\text{sec}}, \tag{A.12}$$

the error is less than 9%.

The base shear forces are calculated by Eqs. (34) and (36) which are $V_{z2} = 1084.2$ kN and $V_{z3} = 225.32$ kN. The ETABS code results in $V_{z2} = 1254.03$ kN and $V_{z3} = 220.43$ kN. The error of the approximate method is less than 14%.

The torque in the second mode is (Eqs. (34) and (36)) $V_{\omega 2} = 7394.3$ kN m. The ETABS code results in $V_{z2} = 7889.77$ KNm, the error of which is less than 7%. The calculated torque cause more than 40% increase in the forces of the outermost load-resisting subsystems. According to EC-8 the torque may also be calculated—as an approximation—by multiplying the shear force (Eq. (A.9)) by 5% of the size of the building (and hence the torsional vibration is not needed to be considered). However this calculation yields $V_{\omega 2} = 2620.6$ kN m which is only 35% of the above calculated value, and hence the approximation suggested by EC-8 is not conservative.

A.2. Unsymmetrical building

We now consider the building given in Fig. 8. In this example we wish to demonstrate the robustness of the approximate calculation. The geometric and material characteristics of the structure are given in Table 4 and Fig. 8.

The same steps are followed as in Appendix A.1.

Step 1. In the longitudinal, y direction the building structure is stiffened by four shear walls ($k = 1, 2, 3, 4$). In the x direction the stiffening system consists three shear walls ($k = 5, 6, 7$) and two coupled shear walls ($k = 8, 9$). The replacement stiffnesses of the lateral load-resisting subsystems are (Köpecsiri and Kollár, 1999a)

$$D_{lk} \approx 0, \quad k = 1, 2, 3, 4, 5, 6, 7,$$

$$D_{lk} = 2E^{w}I^{wb} = 3.45 \times 10^{8}\ \mathrm{kN\,m^2}, \quad k = 8, 9,$$

$$D_{0k} = E^{w}I^{wb} = 1.725 \times 10^{8}\ \mathrm{kN\,m^2}, \quad k = 1, 2, 3, 4, 5, 6, 7,$$

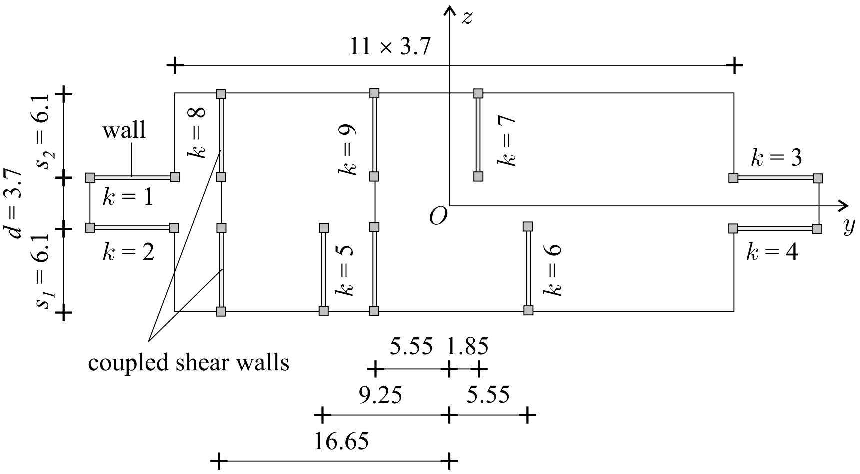

Fig. 8. Numerical example of Appendix A.2.

Table 4
Geometric and material characteristics of the shear walls (see Figs. 7 and 8)

Number of stories	28
Story height, h	2.97 m
Total height, H	83.2 m
Mass/unit height, m	280 640 kg/m
Mass moment of inertia/unit height, θ	69 001 kg m^2/m
Young's modulus of walls, E^{w}	1.95×10^{7} kN/m^2
Young's modulus of beams, E_b	2.3×10^{7} kN/m^2
Shear modulus of beams, G_b	9.58×10^{6} kN/m^2
Area of beams, A_b	0.07 m^2
Moment of inertia of beams, I_b	5.79×10^{-4} m^4
Area of walls, A^{wa} (in Appendix A.1)	1.4640 m^2
Moment of inertia of walls, I^{wa} (in Appendix A.1)	4.5396 m^4
Area of walls, A^{wb} (in Appendix A.2)	2.158 m^2
Moment of inertia of walls, I^{wb} (in Appendix A.2)	8.85 m^4

$$D_{0k} = 2E^{w}A^{wb}(c^{w})^{2} = 2.02 \times 10^{9}\ \mathrm{kN\,m^{2}}, \quad k = 8, 9,$$

$$S_k \approx \infty, \quad k = 1, 2, 3, 4, 5, 6, 7,$$

$$S_k = \left(\left(\frac{6E_bI_b 2(d+s_1)^2}{d^3h\left(1+\frac{12\rho E_bI_b}{G_bd^2A_b}\right)} \right)^{-1} + \left(2\frac{12E^{w}I^{wb}}{h^2} \right)^{-1} \right)^{-1} = 9.99 \times 10^{4}\ \mathrm{kN}, \quad k = 8, 9.$$

Step 2. The stiffnesses in the global coordinate system are (Potzta, 2002):

$$[D_l]_k = D_{lk}[R]_k, \quad [D_0]_k = D_{0k}[R]_k, \quad [S]_k = S_k[R]_k, \tag{A.13}$$

where

$$[R]_k = \begin{bmatrix} \cos^2\alpha_k & -\cos\alpha_k\sin\alpha_k & r_k\cos\alpha_k \\ -\cos\alpha_k\sin\alpha_k & \sin^2\alpha_k & -r_k\sin\alpha_k \\ r_k\cos\alpha_k & -r_k\sin\alpha_k & r_k^2 \end{bmatrix}. \tag{A.14}$$

In the y direction $\alpha_k = 0$ ($k = 1, 2, 3, 4$), in the x direction $\alpha_k = \pi/2$ ($k = 5, 6, 7, 8, 9$), r_k is the distance of the kth lateral load-resisting subsystem to the origin of the global coordinate system (Fig. 8):

k	1	2	3	4	5	6	7	8	9
r_k	1.85	−1.85	1.85	−1.85	−9.25	5.55	1.85	−16.65	−5.55

For $l_0 = 2H$ the replacement stiffness matrices of the structure are (Eq. (6)):

$$[A] = \sum_{k=1}^{16}\left(\frac{D_{0k}}{1+\frac{\pi^2 D_{0k}}{l_0^2 S_k}} + D_{lk} \right) = \begin{bmatrix} \varepsilon & 0 & 0 \\ 0 & 8.171\times10^{13} & -9.069\times10^{14} \\ 0 & -9.069\times10^{14} & 1.258\times10^{16} \end{bmatrix},$$

$$[B] = \sum_{k=1}^{16}\pi^2\left([E] + \frac{\pi^2}{l_0^2}[D_0]_k[S]_k^{-1} \right)^{-1}[D_0]_k[S]_k^{-1}\left([E] + \frac{\pi^2}{l_0^2}[D_0]_k[S]_k^{-1} \right)^{-1}[D_0]_k$$
$$= \begin{bmatrix} \varepsilon & 0 & 0 \\ 0 & 1.652\times10^{18} & -1.834\times10^{19} \\ 0 & -1.834\times10^{19} & 2.544\times10^{20} \end{bmatrix},$$

$$[C] = \tag{A.15}$$

$$[D_0] = [A][B]^{-1}[A] = \begin{bmatrix} \varepsilon & 0 & 0 \\ 0 & 4.041\times10^{9} & -4.486\times10^{10} \\ 0 & -4.486\times10^{10} & 6.223\times10^{11} \end{bmatrix},$$

$$[S] = [A][B]^{-1}[A][B]^{-1}[A] = \begin{bmatrix} \varepsilon & 0 & 0 \\ 0 & 1.999\times10^{5} & -2.219\times10^{6} \\ 0 & -2.219\times10^{6} & 3.078\times10^{7} \end{bmatrix},$$

$$[D_l] = \sum_{k=1}^{16}([D_0]_k + [D_l]_k) - [D_0] = \begin{bmatrix} 6.876\times10^{8} & 0 & 0 \\ 0 & 1.208\times10^{9} & -70.978\times10^{9} \\ 0 & -70.978\times10^{9} & 1.293\times10^{11} \end{bmatrix}.$$

We note that some of the stiffness matrices are singular because they contain a zero element in the main diagonal. For numerical purpose we replaced the zero elements in the main diagonal by a small element ε ($\varepsilon > 0$). (We have chosen the value of ε equal to the smallest element of the main diagonal divided by 10^3.)

Step 3. The natural frequencies are calculated from Eq. (14)

$$\left[\left(\frac{H^4}{\mu_{Bi}^2}[D_0]^{-1}+\frac{H^2}{\mu_{Si}^2}[S]^{-1}\right)^{-1}+\frac{\mu_{Bi}^2}{H^4}[D_1]-\omega_{mi}^2 m[M]\right]\left\{\begin{matrix} v_{0m} \\ w_{0m} \\ \psi_{0m}\end{matrix}\right\}=0, \tag{A.16}$$

where $[M]$ is a diagonal matrix

$$[M]=\begin{bmatrix} 1 & 0 & 0 \\ 0 & 1 & 0 \\ 0 & 0 & \frac{\theta}{m}\end{bmatrix}=\begin{bmatrix} 1 & 0 & 0 \\ 0 & 1 & 0 \\ 0 & 0 & 159.09\end{bmatrix}.$$

By substituting $\mu_{B1}=3.52$, $\mu_{S1}=0.5\pi$ (Table 2) into Eq. (A.16) we obtain the following three eigenvalues:

$$\omega_{m1}^2=1.981,\quad \omega_{m2}^2=0.635,\quad \omega_{m3}^2=0.352.$$

The following three eigenvalues are obtained by substituting $\mu_{B2}=22.03$, $\mu_{S2}=1.5\pi$ (Table 2). Eq. (A.16) results in

$$\omega_{m4}^2=64.61,\quad \omega_{m5}^2=24.86,\quad \omega_{m6}^2=12.87.$$

The modes 7–9 are obtained by introducing $\mu_{B3}=61.7$, $\mu_{S3}=2.5\pi$ into Eq. (A.16) which yield

$$\omega_{m7}^2=486.02,\quad \omega_{m8}^2=195.02,\quad \omega_{m9}^2=99.44.$$

The periods of vibration, T are

$$T_i=\frac{2\pi}{\omega_i}. \tag{A.17}$$

The results of the approximate calculation and those of the ETABS code are given in Table 5. The maximum error is −10%.

Step 4. The base shear forces are calculated by Eq. (34). The structure has one plane of symmetry (x–y), thus from the lateral vibration in the x–y plane base shear force arises only in the y direction. However from the lateral (x–z)–torsional vibration both a shear force and a torque arise. The base overturning moments are calculated from Eq. (37). The internal forces in the first three modes in case of different earthquake excitations are given in Table 6. Table 6 also contains the results of the ETABS calculation, and the errors of the approximation.

The design value of the internal forces can be calculated by combining the modal responses (Eurocode 8):

Table 5
Comparison of the numerical and approximate results for the periods of vibration, (T), and the spectral accelerations, S_{ei}

Mode	Direction	Period of vibration, T (s)		Error [%]	S_{ei}
		Approximation	ETABS		
1	Lateral (x–z)–torsional	10.59	10.53	0.57	0.0416
2	x–y plane	7.89	8.26	−4.69	0.0751
3	Lateral (x–z)–torsional	4.46	4.32	3.24	0.234
4	Lateral (x–z)–torsional	1.75	1.86	−5.41	0.889
5	x–y plane	1.26	1.35	−6.67	1.24
6	Lateral (x–z)–torsional	0.78	0.83	−6.02	1.99
7	Lateral (x–z)–torsional	0.63	0.70	−10.0	2.47
8	x–y plane	0.45	0.50	−10.0	2.60
10	Lateral (x–z)–torsional	0.29	0.32	−9.38	2.60

Table 6
Internal forces

Mode	Excitation	Internal force	Approximation	ETABS	Error [%]
2 (x–y plane)	x–y	V_y [kN]	1070	998.8	7.13
		M_y [kN m]	65 635	61 147	7.34
3 (x–z plane-torsional)	x–z	V_z [kN]	2175	2170	0.26
		V_ω [kN m]	22 031	22 674	−2.84
		M_z [kN m]	129 450	132 772	−2.50
1 (x–z plane-torsional)	x–z	V_z [kN]	223.6	253.7	−11.87
		V_ω [kN m]	3839	3383	8.39
		M_z [kN m]	13 879	15 496	−10.43
5 (x–y plane)	x–y	V_y [kN]	5423	5232	3.65
		M_y [kN m]	93 549	90 810	3.02
6 (x–z plane-torsional)	x–z	V_z [kN]	5415.8	5008	8.14
		V_ω [kN m]	50 927	48 072	5.94
		M_z [kN m]	93 333	89 190	4.64
4 (x–z plane-torsional)	x–z	V_z [kN]	1432	1464	−2.20
		V_ω [kN m]	22 989	21 037	9.28
		M_z [kN m]	24 711	25 987	−4.91
8 (x–y plane)	x–y	V_y [kN]	3938	4026	−2.20
		M_y [kN m]	41 561	41 704	−0.34
10 (x–z plane-torsional)	x–z	V_z [kN]	2512	2561	−1.90
		V_ω [kN m]	23 428	23 363	0.28
		M_z [kN m]	26 543	26 812	−1.00
7 (x–z plane-torsional)	x–z	V_z [kN]	1338.8	1336	0.22
		V_ω [kN m]	22 401	19 467	15.07
		M_z [kN m]	14 124	14 350	−1.57

$$\{V\} = \sum_1^9 \sqrt{\{V_i^2\}} = \begin{Bmatrix} 6786 \\ 6659 \\ 68\,358 \end{Bmatrix}, \quad \{M\} = \sum_1^9 \sqrt{\{M_i^2\}} = \begin{Bmatrix} 121\,601 \\ 164\,850 \end{Bmatrix}.$$

The ETABS calculation gives

$$\{V\} = \sum_1^9 \sqrt{\{V_i^2\}} = \begin{Bmatrix} 6677 \\ 6351 \\ 64\,837 \end{Bmatrix}, \quad \{M\} = \sum_1^9 \sqrt{\{M_i^2\}} = \begin{Bmatrix} 118\,173 \\ 165\,600 \end{Bmatrix}.$$

The maximum error is 5.43%. Including 15 modes in the ETABS calculation the design values of the base shear force are

$$V_y = \sum_1^{15} \sqrt{V_y^2} = 7050 \text{ kN},$$

$$V_z = \sum_1^{15} \sqrt{V_z^2} = 6500 \text{ kN},$$

which result less than 4% error.

References

Basu, A.K., 1983. Seismic design charts for coupled shear walls. J. Struct. Eng., ASCE 109 (2), 335–352.
Basu, A.K., Nagpal, A.K., Kaul, S., 1984. Charts for seismic design of frame-wall systems. J. Struct. Eng., ASCE 110 (1), 31–46.
Beck, H., 1962. Contribution to the analysis of coupled shear walls. J. Am. Conc. Inst. 55, 1055–1069.
Bishop, R.E.D., Jonson, D.C., 1960. The Mechanics of Vibration. Cambridge University Press, London. pp. 233–239.
Chopra, A.K., 1995. Dynamics of Structures: Theory and application to Earthquake Engineering. Prentice Hall, New Yersey. pp. 434–438, 468–519.
Dunkerley, S., 1984. On the whirling and vibration of shafts. Philos. Trans. R. Soc. A. 185, 279–360.
Eurocode 8. Design provisions for earthquake resistance of structures.
Hegedűs, I., Kollár, L.P., 1999. Application of the sandwich theory in the stability analysis of structures. In: Kollár, L. (Ed.), Structural Stability in Engineering Practice. Spon, London.
Kollár, L., Iványi, G., 1966. Kippen und Biegedrillknicken von Schalenbogen mit Hilfe der Energiemethode. Bautechnik-Archiv, W. Ernst und Sohn, Berlin, Munchen, H.19.
Kollár, L.P., 1991. Calculation of plane frames braced by shear walls for seismic load. Acta Tech., Acad. Sci. Hung., Budapest 104 (1–3), 187–209.
Kollár, L.P., 2001. Flexural–torsional vibration of open section composite beams with shear deformation. Int. J. Solids Struct. 38, 7543–7558.
Köpecsiri, A., Kollár, L.P., 1999a. Approximate seismic analysis of building structures by the continuum method. Acta Tech., Civil Eng., Budapest 108 (3–4), 417–446.
Köpecsiri, A., Kollár, L.P., 1999b. Simple formulas for the analysis of symmetric (plane) bracing structures subjected to earthquakes. Acta Tech., Civil Eng., Budapest 108 (3–4), 447–473.
Köpecsiri, A., 1997. Approximate seismic analysis of building structures by the continuum method. Ph.D. Thesis. Technical University of Budapest, Budapest.
Lamb, H., Southwell, R.V., 1921. The vibration of a spinning disk. Proc. R. Soc. A. 99, 272–280.
Ng, S.C., Kuang, J.S., 2000. Triply coupled vibration of asymmetric wall-frame structures. J. Struct. Eng., ASCE 126 (8), 982–987.
Potzta, G., Kollár, L.P., 2003. Analysis of building structures by replacement sandwich beams. Int. J. Solids Struct. 40, 535–553.
Potzta, G., 2002. Approximate analysis of building structures subjected to earthquakes. Ph.D. Thesis. Technical University of Budapest, Budapest.
Rosman, R., 1973. Dynamics and stability of shear wall building structures. Proc. Instn. Civil Engs. 55, 411–423.
Rosman, R., 1974. Stability and dynamics of shear wall frame structures. Build. Sci. 9, 55–63.
Rutenberg, A., 1975. Approximate natural frequencies for coupled shear walls. Earthquake Eng. Struct. Dynam. 4, 95–100.
Rutenberg, A., 1979. An accurate approximate formula for the natural frequencies of sandwich beams. Comput. Struct. 10, 875–878.
Skattum, S.K., 1971. Dynamic analysis of coupled shear walls and sandwich beams. Ph.D. Thesis. California Institute of Technology.
Stafford Smith, B., Coull, A., 1991. Tall Building Structures: Analysis and Design. John Wiley and Sons, Inc., New York.
Stafford Smith, B., Crowe, E., 1986. Estimating periods of vibration of tall buildings. J. Struct. Eng., ASCE 112 (5), 1005–1019.
Stafford Smith, B., Yoon, Y.S., 1991. Estimating seismic base shears of tall wall-frame buildings. J. Struct. Eng., ASCE 117 (10), 3026–3041.
Szerémi, L., 1978. Stiffening system of multistory buildings by the continuum model. Periodica Politech. Civil Eng. 22 (3–4), 205–218.
Tarnai, T., 1999. Summation theorems. In: Kollár, L. (Ed.), Structural Stability in Engineering Practice. Spon, London.
Zalka, K.A., 1993. An analytical procedure for 3-dimensional eigenvalue problems. Building Research Establishment Note. 32/93.
Zalka, K.A., 1994. Dynamic analysis of core supported buildings. Building Research Establishment Note. 127/94.
Zalka, K.A., 2000. Global Structural Analysis of Buildings. E&FN Spon, London.
Zalka, K.A., 2001. A simplified method for calculation of the natural frequencies of wall-frame buildings. Eng. Struct. 23, 1544–1555.